Contract No:

This document was prepared in conjunction with work accomplished under Contract No. DE-AC09-08SR22470 with the U.S. Department of Energy (DOE) Office of Environmental Management (EM).

Disclaimer:

SRNL-STI-2016-00060

Keywords: *Mechanical Properties, Type 304L Stainless Steel, Type 316L Stainless Steel, Type 21-6-9 Stainless Steel, Hydrogen Embrittlement, J-Integral, Helium Embrittlement, Forging*

Retention: *Permanent*

2015 Accomplishments – Tritium Aging Studies on Stainless Steel: Effects of Hydrogen Isotopes, Crack Orientation, and Specimen Geometry on Fracture Toughness

MICHAEL J. MORGAN
Materials Science and Technology

Publication Date: January 2016

This document was prepared in conjunction with work accomplished under Contract No. DE-AC09-08SR22470 with the U. S. Department of Energy

Savannah River National Laboratory
Savannah River Nuclear Solutions, LLC
Aiken, SC 29808

Prepared for the U.S. Department of Energy under contract number DE-AC09-08SR22470.

Printed in the United States of America

Prepared for
U.S. Department of Energy

2015 Accomplishments – Tritium Aging Studies on Stainless Steel: Effects of Hydrogen Isotopes, Crack Orientation, and Specimen Geometry on Fracture Toughness

CONTENTS **PAGE**

List of Figures **Page**

List of Tables

EFFECTS OF HYDROGEN ISOTOPES, CRACK ORIENTATION AND SPECIMEN GEOMETRY ON FRACTURE TOUGHNESS

I. SUMMARY

Forged stainless steels have long been used as the materials of construction for tritium reservoirs. These steels are highly resistant to, but not immune from, the embrittlement effects of tritium and its radioactive decay product, helium-3. Tritium embrittlement can occur after long term tritium service after tritium has diffused into the reservoir walls. It is another manifestation of hydrogen embrittlement that is made worse by the presence of tritium's radioactive decay product, helium-3. The factors that affect the tendency for crack formation and propagation are the subject of this investigation and include: tritium exposure history, steel composition and microstructure; and vessel configuration (geometry, pressure, residual stress). Fracture mechanics is one of the chief analytical methods for evaluating the long-term effects of tritium on the structural properties of reservoirs and those analyses require fracture toughness data. Experimental research programs are underway and are designed to measure tritium and decay helium effects on the cracking properties of stainless steels using actual tritium reservoir forgings instead of the experimental forgings of past programs (1). The properties measured are expected to be more representative of actual reservoir properties because the microstructure of the specimens tested will be more like that of the tritium reservoirs. In FY15, the fracture toughness properties of Type 316L and two heats of Type 304L stainless steels were reported for Stem, Cup and Block forgings before and after exposure hydrogen gas (2). A series of tritium exposures over the last few years was completed during FY15 and specimen aging is underway to build in decay helium. Fracture toughness testing for short and long age conditions will be started during FY16. Also, the Hydrogen Fracture Toughness Tester was completed for conducting fracture toughness tests in high pressure hydrogen gas (3).

This study reports on the effects of hydrogen isotopes, crack orientation, and specimen geometry on the fracture toughness of stainless steels. Fracture toughness variability was investigated for Type 21-6-9 stainless steel using the 7K0004 forging. Fracture toughness specimens were cut from the forging in two different geometric configurations: arc shape and disc shape. The fracture toughness properties were measured at ambient temperature before and after exposure to hydrogen gas and compared to prior studies. There are three main conclusions that can be drawn from the results. First, the fracture toughness properties of actual reservoir forgings and contemporary heats of steel are much higher than those measured in earlier studies that used heats of steel from the 1980s and 1990s and forward extruded forgings which were designed to simulate reservoir microstructures. This is true for as-forged heats as well as forged heats exposed to hydrogen gas. Secondly, the study confirms the well-known observation that cracks oriented parallel to the forging grain flow will propagate easier than those oriented perpendicular to the grain flow. However, what was not known, but is shown here, is that this effect is more pronounced, particularly after hydrogen exposures, when the forging is given a larger upset. In brick forgings, which have a relatively low amount of upset, the fracture toughness variation with specimen orientation is less than 5%; whereas, in cup forgings, the fracture toughness is about 20% lower than that

measured for specimens taken from the stem section. Finally, this study used the 7K0004 forging to show how specimen geometry affects fracture toughness values. The American Society for Testing Materials (ASTM) specifies minimum specimen section sizes for valid fracture toughness values. However, sub-size specimens have long been used to study tritium effects because of the physical limitation of diffusing hydrogen isotopes into stainless steel at mild temperatures so as to not disturb the underlying forged microstructure. This study shows that fracture toughness values of larger specimens are higher and more representative of the material's fracture behavior in a fully constrained tritium reservoir. The toughness properties measured for sub-size specimens were about 65-75% of the values for larger specimens. While the data from sub-size specimens are conservative, they may be overly so. The fracture toughness properties from sub-size specimens are valuable in that they can be used for tritium effects studies and show the same trends and alloy differences as those seen from larger specimen data. Additional work is planned, including finite element modeling, to see if sub-size specimen data could be adjusted in some way to be more closely aligned with the actual material behavior in a fully constrained pressure vessel.

This report fulfills the requirements for a portion of the Enhanced Surveillance Program FY16 Level 2 milestone 5649 to "provide input to the Laboratories in the form of technical reports on significant ESC results for informing the stockpile decisions."

II. INTRODUCTION

Tritium reservoirs have long been fabricated from forged stainless steels and filled and stored at the Savannah River Site. The vessels are constructed from forged stainless steels because of their good compatibility with tritium. These steels are highly resistant to, but not immune from, the embrittling effects of hydrogen isotopes and helium from tritium decay. Cracking in storage vessels has been observed after extended service times and material properties like ductility, elongation-to-failure, and fracture toughness are reduced with time as tritium and its radioactive decay product, He^3, slowly accumulate within the vessel walls during service (4-13). One of the primary interests of the Savannah River Site's Enhanced Surveillance Program is to provide data on tritium effects on steel behavior and fracture toughness values for use by the Design Agencies for fracture modeling, reservoir life prediction, and safety margin evaluations (4 - 24).

New experimental research and development programs are underway and were described in a recent report (1). These programs are first-of-a-kind because they set out to measure tritium and decay helium effects on the cracking properties of stainless steels using actual tritium reservoir forgings instead of the experimental forgings of past programs (7,15). In this way, the properties measured will be more representative of actual reservoir properties because the microstructure of the specimens will be more like that of the forged reservoirs. The test matrices for the various programs are designed to measure the effects of specific forging variables on tritium compatibility and were described earlier (1). The programs include three heats of stainless steel, multiple yield strengths, four different forging processes, and four different reservoir forgings.

In last year's report (2), the fracture toughness properties of Type 316L and two heats of Type 304L stainless steels were shown for Stem, Cup and Block forgings before and after exposure hydrogen gas. For type 316L forgings, the properties were measured for specimens cut in two different orientations from the stem and cup portions of the forging. A series of tritium exposures over the last few years was completed during FY15 and specimen aging is underway to build in decay helium effects. Fracture toughness testing for a short and long age condition will be started during FY16. Future testing will take advantage of the new Hydrogen Fracture Toughness Tester which was completed in FY15 for conducting fracture mechanics tests in high pressure hydrogen gas.

In this report, fracture toughness variability was investigated for the Type 21-6-9 stainless steel 7K0004 forging. Part-to-part and within-part toughness variability was measured as well as the effects of crack orientation and hydrogen exposure. A second purpose was to conduct fracture toughness testing using two different specimen geometries – arc-shaped specimens and compact-disc shaped specimens. The results will be compared to results Melcher of Los Alamos National Laboratory (LANL) who conducted fracture toughness measurements on larger compact-tension specimens taken from a similar forging (25).

The LANL Brick forging offers several advantages for fracture mechanics studies on stainless steels. First of all, the forging, unlike most reservoir forgings, is large enough so that full-size fracture mechanics specimens can be machined from it as well as the sub-size samples that have been commonly used in hydrogen and tritium compatibility studies. Sub-size samples are used for hydrogen embrittlement studies because of physical limitations associated with diffusing hydrogen into large sections in reasonable times at mild temperatures without changing material microstructure. However, fracture toughness properties can be sample-size dependent because the crack tip is not as constrained as it would be in the actual structure; i.e., a pressure vessel. Cracks that may form within the wall of a tritium reservoir are fully constrained (i.e. surrounded by elastically strained material). The spherical or cylindrical geometry of the reservoir limits any contraction of the stressed material surrounding the crack which keeps stress levels at the crack tip high. ASTM specifies minimum specimen section sizes for valid fracture toughness values to ensure that the stress and strain levels near the crack tip in the specimen under test are not relaxed by plastic deformation and contraction of the surrounding material and are similar to those expected in a fully constrained structure. Quantification of the specimen geometries used for hydrogen and tritium embrittlement studies have not been carefully examined until now.

III. EXPERIMENTAL PROCEDURE

The compositions of the stainless steels used in this and the earlier studies (1-2) are shown in Table I and the mechanical properties are shown in Table II. Two fracture toughness specimens were fabricated from the forgings – arc-shaped and disk-shaped – shown in Figure 1. Figure 2 shows the brick-shaped Type 21-6-9 7K0004 forging. Fracture toughness variation within the part was examined by sectioning the forging into several numbered slabs from top to bottom and cutting out fracture toughness specimens from two different orientations, LT and TL, as shown in Figures 3 and 4. LT specimens

are loaded in the longitudinal direction and have cracks propagating transverse to grain flow.TL specimens are loaded in the transverse direction and have cracks propagating parallel to grain flow. Fracture toughness properties were measured for two heats of the forging before and after exposure to hydrogen gas described below. Tritium exposure will be planned at a later date after the property variations within the forging have been better characterized. Tables VI, VII, and VIII list the samples that were cut from the two forging heats and their test conditions – not charged or hydrogen charged.

Table I - Compositions and Mechanical Properties of Types 316L, 304L and 21-6-9 Stainless Steel Forgings (Weight %)

Material	MCN*	Heat	Cr	Ni	Mn	P	Si	Co	Mo	C	S	N	O	Al
304L Block LY	200952	11459	18.6	9.5	1.7	-	.57	.061	.098	.022	.001	-	-	-
304L Block HY	200952	11460	18.6	9.5	1.7	-	.57	.061	.098	.022	.001	-	-	-
316L Cup	200948	7K0010	16.6	12.9	.71	.011	.51	.029	2.3	.009	.004	.036	.001	.003
21-6-9 Brick	200787	13680	21.0	7.3	9.2	.015	.52	-	-	0.03	.0005	.280	.002	.020
21-6-9 Brick	200681	12353	19.3	7.2	9.1	.019	.44	-	-	0.03	.001	.300	.005	.024

***MCN (Material Control Number)**

Table II Ambient Temperature Mechanical Properties of Stem, Cup, Block and Brick Forgings

Material	MCN*	Forging / Direction	Yield Strength ksi	Ultimate Strength ksi	Elongation %
316L Stem	200948	7K0010 – Longitudinal	52.8	83.3	52.0
316L Stem	200948	7K0010 - Cylindrical	57.7	88.5	60.7
316L Cup	200948	7K0010 - Longitudinal	71.9	98.3	50.8
304L Block LY	200952	11459 - Longitudinal	59.9	89.4	67.6
304L Block LY	200952	11459 - Cylindrical	60.4	95.3	58.1
304L Block HY	200952	11460 - Longitudinal	67.5	93.9	56.8
304L Block HY	200952	11460 - Cylindrical	71.7	101.9	53.5
21-6-9 Brick	200787	7K0004	63.0	108	47.2
21-6-9 Brick	200681	7K0004	64.9	108	51.4

***MCN (Material Control Number)**

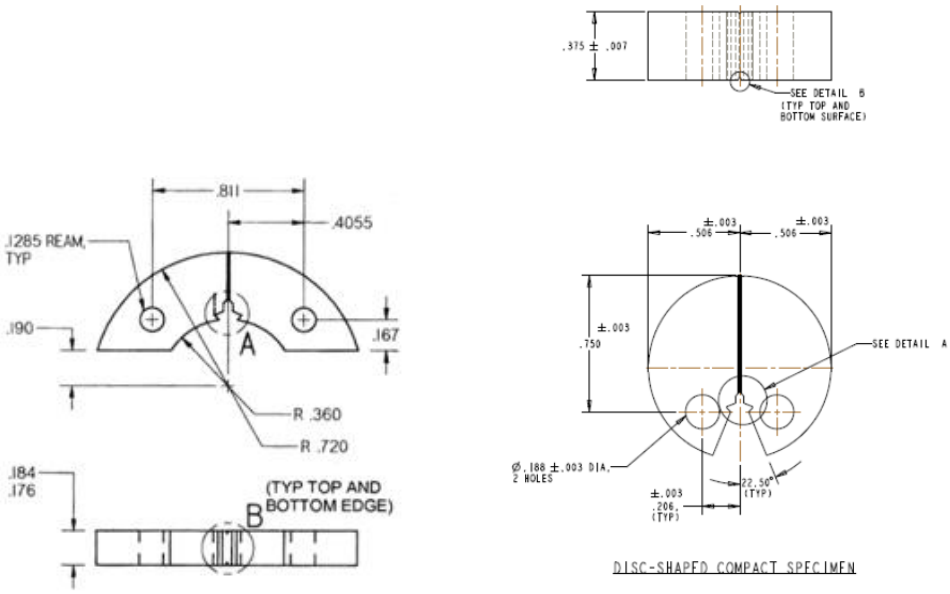

Figure 1. Fracture Toughness Specimens: (a) Arc-Shaped; and, (b) Disk-Shaped. Dimensions are in Inches.

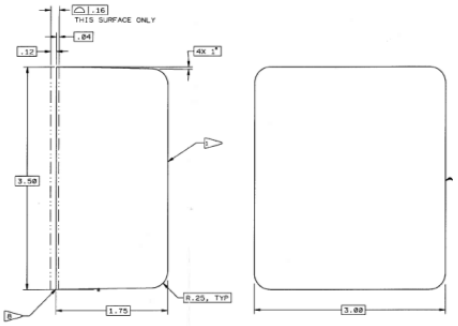

Figure 2. LANL Type 21-6-9 Brick Forging 7K0004. Dimensions are in Inches.

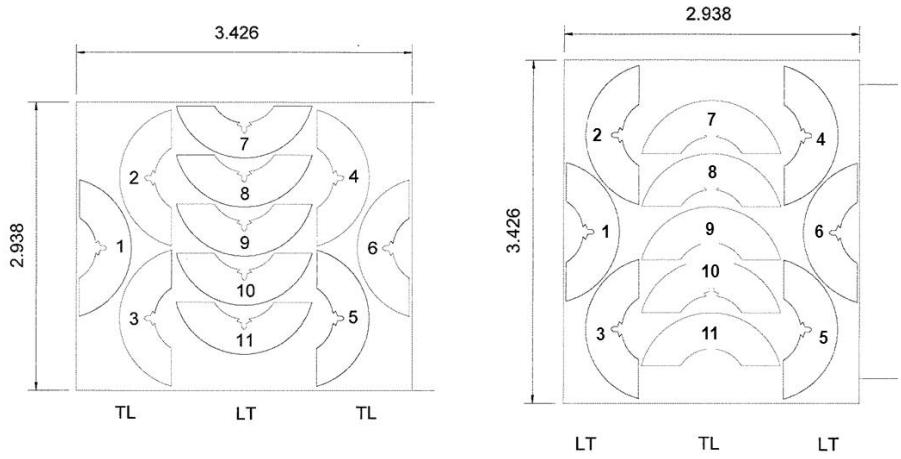

(a) Odd Numbered Slabs (1,3,5,7) **(b) Even Numbered Slabs (2,4,6)**

Figure 3. Location and Orientation of Arc-Shaped Fracture Toughness Specimens in a Typical Layer for 7K0004 Forging. Dimensions are in Inches.

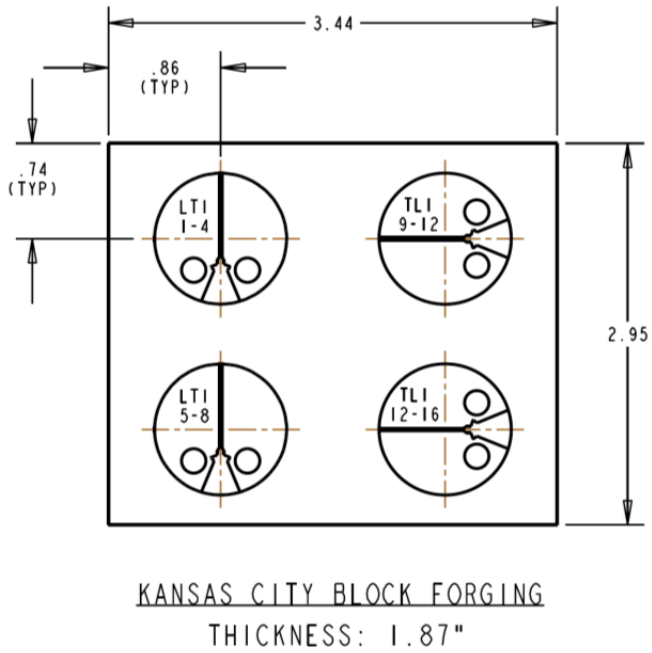

Figure 4. (a) Disc-Shape Fracture Toughness Specimen Showing Location and Orientation Within 7K0004 Forging. Dimensions are in Inches.

Figure 5 shows the Type 316L stainless steel in the form of a cylindrical-cup forging and Figure 6 shows the Type 304L stainless steel forgings in the form of two cylindrical blocks. Figure 5 also shows how arc-shaped specimens were cut from the Type 316L stainless steel in the CR-orientation and from the stem in the CL-orientation. Cracks run in the radial direction for the CR specimens and in the longitudinal direction for the CL specimens. The arc specimen geometry is shown in Figure 1. Arc-shaped specimens were cut from two Type 304L stainless steel cylindrical block forgings shown in the drawing in Figure 6. The Type 304L stainless steel forgings were produced to have two different yield strengths: nominally, 60 ksi and 70 ksi. The orientation and location of the fracture toughness specimens cut from the block forgings is shown in Figure 6. Additional details and results of the test matrices for the stem, cup, and block forging studies including tritium pre-charging schedules and experimental plans are given in the technology development plan (1-2).

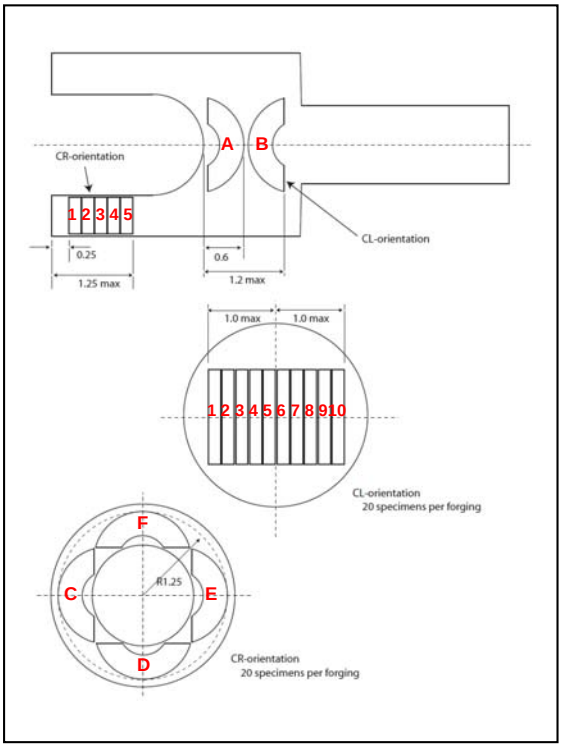

Figure 5. Fracture Toughness Specimen Location and Orientation - Type 316L Forging: Specimens Labeled “A” or “B” were Cut from the Stem Portion of the Forging and Specimens Labeled “C”, “D”, “E”, or “F” from the Cup Portion of the Forging. Dimensions are in Inches.

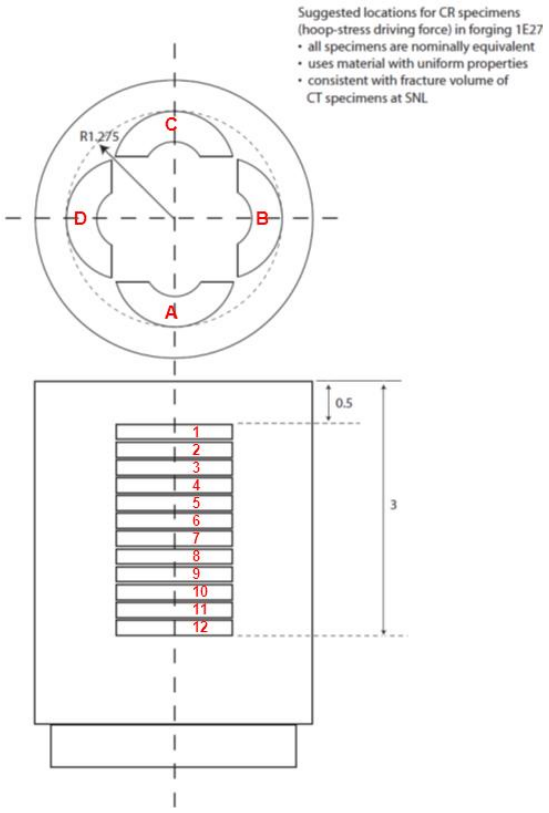

Figure 6. Fracture Toughness Specimen Location and Orientation For Type 304L Cylindrical Block Forging.

Selected specimens cut from the Types 21-6-9, 316L, and 304L block forgings were pre-charged with hydrogen or tritium gas (for Types 316L and 304L) at 350 C and an over-pressure of 5000 psi and then stored in air at -50 C. The storage temperature was chosen so as to minimize tritium off-gassing loss and to allow for the build-in of helium from tritium decay until testing is performed (this process sometimes takes years to accomplish). Tritium-exposed specimens are scheduled to be tested during FY16. The hydrogen isotope content of the pre-charged specimens is estimated by using established hydrogen solubility values to be 3700 atomic parts per million (appm) for Types 304L and 316L stainless steels (26). Tables III through VII list the specimen and specific hydrogen or tritium exposures and test environments.

J-integral tests were conducted at room temperature in air using a screw-driven testing machine and a crosshead speed of 0.005 in/min while recording load, load-line displacement with a gage clipped to the crack mouth, and crack length (Figure 7). Crack length was monitored using a DC potential drop system and guidelines described in ASTM E647-95 (27). The J-Integral versus crack length increase (J-R) curves were constructed from the data using ASTM E1820-99 (28). Fracture toughness values are determined by using the intercept of an offset line with the J-R curve as shown in Figure 8 which shows data on the effect of tritium from an earlier study (15). The offset line has a slope that is proportional to the flow strength of the material. As the material yields before cracking the crack tip blunts and changes shape. In effect, the ASTM procedure is

determining the point at which the crack begins to grow after blunting has occurred. The slope of the blunting line in the standard is generally taken to between 4/3 and 2 times the material's flow strength based on best fits to numerous alloys. The flow strength is defined as the average between yield and ultimate strengths. This study included materials having a range of flow strengths with an overall average of 80 ksi. For the Stem, Cup, Block and Brick forgings, the best-fit slope for the blunting line was (2.5 x Flow Strength). These best-fit values were used to determine fracture-toughness values to avoid later complications in the analysis because hydrogen, tritium, and decay helium all affect flow strength, and tensile specimens would not be available for each condition. The blunting lines are shown for the J-R Curve results to show the goodness of fit to the data. No attempt was made at this time to quantify the fracture toughness differences as a function of blunting-line slope. In general, fracture toughness values determined with steeper sloped blunting lines are lower and therefore, more conservative. In these high work-hardenable stainless steels, the J-R curve clearly deviates away from the lower sloped blunting lines as the material in front of the crack work hardens prior to crack extension. Because of this, the fracture toughness properties reported here will be conservative.

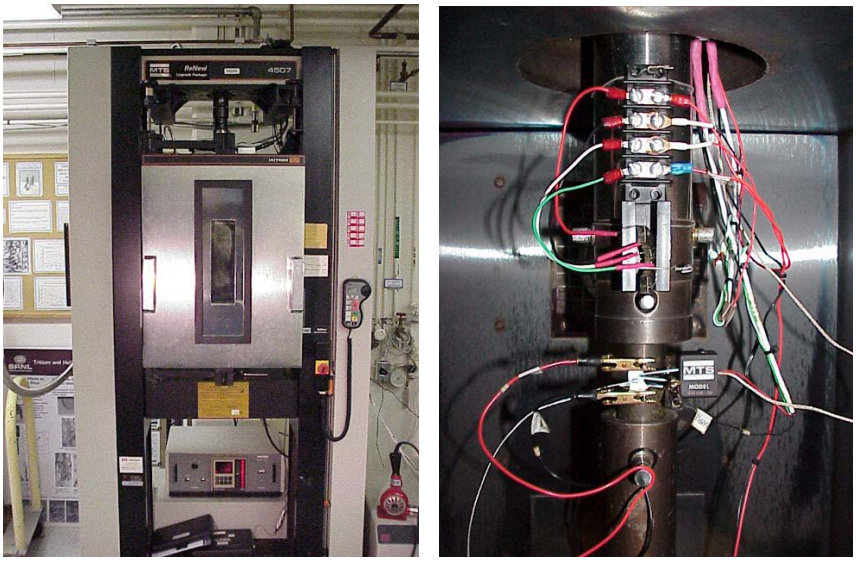

(a) (b)

Figure 7. (a) Mechanical Testing Machine with Environmental Chamber For Non-Charged and Hydrogen-Charged Specimens. (b) Fracture-Toughness Specimen with Crack Length DC Potential Drop Leads and Thermocouple.

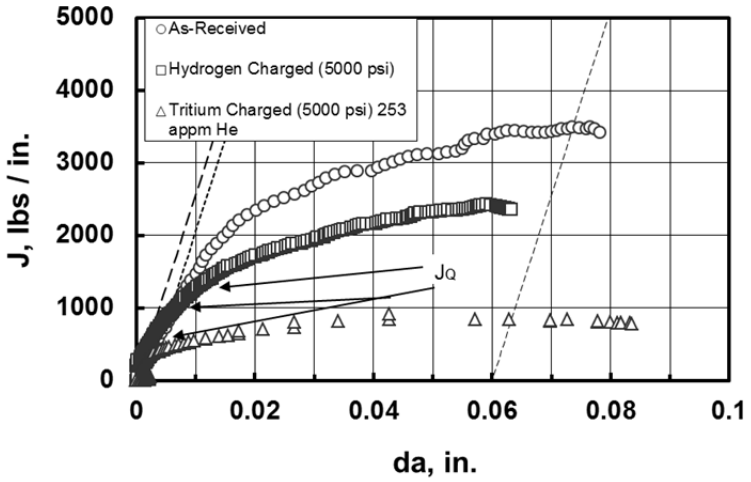

Figure 8. Typical J-R curves for As-received (Not Charged), Hydrogen Pre-charged, and Tritium Pre-charged Type 21-6-9 Stainless Steels. J_Q Values Shown Were Determined from the Intercept of the J-R Curve with the Offset Line (15).

Table III - Type 21-6-9 Brick Forging Sample Test Matrix – MCN 600787

Labeling Scheme: Orientation-Heat-Slab-Sample #
Eg. TL-1-3-5 – TL Orientation, Heat#1, Slab 3, Sample 5

Odd-Numbered Slabs				**Even Numbered Slabs**		
TL Orientation				**LT Orientation**		
TL-1-1-1	TL-1-3-1	TL-1-5-1	TL-1-7-1	LT-1-2-1	LT-1-4-1	LT-1-6-1
TL-1-1-2	TL-1-3-2	TL-1-5-2	TL-1-7-2	LT-1-2-2	LT-1-4-2	LT-1-6-2
TL-1-1-3	TL-1-3-3	TL-1-5-3	TL-1-7-3	LT-1-2-3	LT-1-4-3	LT-1-6-3
TL-1-1-4	TL-1-3-4	TL-1-5-4	TL-1-7-4	LT-1-2-4	LT-1-4-4	LT-1-6-4
TL-1-1-5	TL-1-3-5	TL-1-5-5	TL-1-7-5	LT-1-2-5	LT-1-4-5	LT-1-6-5
TL-1-1-6	TL-1-3-6	TL-1-5-6	TL-1-7-6	LT-1-2-6	LT-1-4-6	LT-1-6-6
LT Orientation				**TL Orientation**		
LT-1-1-7	LT-1-3-7	LT-1-5-7	LT-1-7-7	TL-1-2-7	TL-1-4-7	TL-1-6-7
LT-1-1-8	LT-1-3-8	LT-1-5-8	LT-1-7-8	TL-1-2-8	TL-1-4-8	TL-1-6-8
LT-1-1-9	LT-1-3-9	LT-1-5-9	LT-1-7-9	TL-1-2-9	TL-1-4-9	TL-1-6-9
LT-1-1-10	LT-1-3-10	LT-1-5-10	LT-1-7-10	TL-1-2-10	TL-1-4-10	TL-1-6-10
LT-1-1-11	LT-1-3-11	LT-1-5-11	LT-1-7-11	TL-1-2-11	TL-1-4-11	TL-1-6-11

Table IV - Type 21-6-9 Brick Forging Sample Test Matrix – MCN 600281

TL Orientation	LT Orientation
TL-2-1-1	LT-2-1-1
TL-2-2-1	LT-2-2-1
TL-2-3-1	LT-2-3-1
TL-2-4-1	LT-2-4-1
TL-2-5-1	LT-2-5-1
TL-2-6-1	LT-2-6-1
TL-2-7-1	LT-2-7-1
TL-2-8-1	LT-2-8-1

Table V Type 21-6-9 Brick Forging Sample Pre-Charging Test Conditions

Heat #1 13680	Pre-Charging	Test Environment	Heat #2 12353	Pre-Charging	Test Environment
LT-1-2-2	None	Air	LT-2-3-1	None	Air
LT-1-3-10	None	Air	LT-2-5-1	None	Air
LT-1-3-9	None	Air	LT-2-7-1	None	Air
TL-1-3-2	None	Air	TL-2-1-1	None	Air
TL-1-3-3	None	Air	TL-2-3-1	None	Air
TL-1-3-4	None	Air	TL-2-5-1	None	Air
TL-1-3-8	None	Air	TL-2-7-1	None	Air
TL-1-7-2	None	Air			
TL-1-7-3	None	Air			
TL-1-7-4	None	Air			
LT-1-3-11	Hydrogen	Air	LT-2-4-1	Hydrogen	Air
LT-1-3-7	Hydrogen	Air	LT-2-6-1	Hydrogen	Air
LT-1-7-7	Hydrogen	Air	LT-2-8-1	Hydrogen	Air
LT-1-7-8	Hydrogen	Air	TL-2-2-1	Hydrogen	Air
LT-1-7-9	Hydrogen	Air	TL-2-2-1	Hydrogen	Air
TL-1-3-5	Hydrogen	Air	TL-2-4-1	Hydrogen	Air
TL-1-3-6	Hydrogen	Air	TL-2-6-1	Hydrogen	Air
TL-1-7-1	Hydrogen	Air	TL-2-8-1	Hydrogen	Air

Table VI - Type 316L Cup Forging (50260) Test Matrix

Location	Pre-Charging	Test Env.	No.	ID	ID	ID
Stem	None	Air	4	26AL1	26AL7	26BL9 26BL3
Stem	Hydrogen	Air	3	26AL2	26AL8	26BL4
Stem	Tritium Age 1	Air	3	26AL3	26AL9	26BL5
Stem	Tritium Age 2	Air	3	26AL4	26AL10	26BL6
Stem	Tritium Age 3	Air	3	26AL5	26BL1	26BL7
Stem	Tritium Age 4	Air	3	26AL6	26BL2	26BL8
Stem	None	5 ksi H_2	3	26AL11	26AL17	26BL13
Stem	None	10 ksi H_2	3	26BL10	26BL19	26BL20
Stem	Hydrogen	5 ksi H_2	3	26AL12	26AL18	26BL14
Stem	Tritium Age 1	5 ksi H_2	3	26AL13	26AL19	26BL15
Stem	Tritium Age 2	5 ksi H_2	3	26AL14	26AL20	26BL16
Stem	Tritium Age 3	5 ksi H_2	3	26AL15	26BL11	26BL17
Stem	Tritium Age 4	5 ksi H_2	3	26AL16	26BL12	26BL18
Cup	None	Air	4	26RC1	26RD3	26RE5 26RF4
Cup	Hydrogen	Air	3	26RF2	26RC4	26RD1
Cup	Tritium Age 1	Air	3	26RE3	26RF5	26RC2
Cup	Tritium Age 2	Air	3	26RD4	26RE1	26RF3
Cup	Tritium Age 3	Air	3	26RC5	26RD2	26RE4
Cup	Tritium Age 4	Air	3	26RF1	26RC3	26RD5
Cup	None	5 ksi H_2	3	26RC6	26RD8	26RE10
Cup	None	10 ksi H_2	3	26RE7	26RF9	26RE2
Cup	Hydrogen	5 ksi H_2	3	26RF7	26RC9	26RD6
Cup	Tritium Age 1	5 ksi H_2	3	26RE8	26RF10	26RC7
Cup	Tritium Age 2	5 ksi H_2	3	26RD9	26RE6	26BF8
Cup	Tritium Age 3	5 ksi H_2	3	26RC10	26RD7	26RE9
Cup	Tritium Age 4	5 ksi H_2	3	26RF6	26RC8	26RD10

Table VII - Type 304L Cylindrical Block Forging Test Matrix
Forging: 00011459 (Low Strength) and 00011460 (High Strength)

Forging	Pre-Charging	Test Env.	No.	ID	ID	ID
11459	None	Air	3	59RA8	59RB1	59RD12
11459	None	Air	3	59RA1	59RB6	59RC11
11459	Hydrogen	Air	3	59RD4	59RA9	59RB2
11459	Tritium Age 1	Air	3	59RC7	59RD11	59RA5
11459	Tritium Age 2	Air	3	59RB10	59RC3	59RD8
11459	Tritium Age 3	Air	3	59RA2	59RB7	59RC12
11459	Tritium Age 4	Air	3	59RD5	59RA10	59RB3
11459	None	5 ksi H2	3	59RC8	59RD1	59RA6
11459	None	10 ksi H2	3	59RA4	59BB9	59RC2
11459	Hydrogen	5 ksi H2	3	59RB11	59RC4	59RD9
11459	Tritium Age 1	5 ksi H2	3	59RA3	59RB8	59RC1
11459	Tritium Age 2	5 ksi H2	3	59RD6	59RA11	59RB4
11459	Tritium Age 3	5 ksi H2	3	59RC9	59RD2	59RA7
11459	Tritium Age 4	5 ksi H2	3	59RB12	59RC5	59RD10
11460	None	Air	3	60RA1	60RB6	60RC11
11460	Hydrogen	Air	3	60RD4	60RA9	60RB2
11460	Tritium Age 1	Air	3	60RC7	60RD11	60RA5
11460	Tritium Age 2	Air	3	60RB10	60RC3	60RD8
11460	Tritium Age 3	Air	3	60RA2	60RB7	60RC12
11460	Tritium Age 4	Air	3	60RD5	60RA10	60RB3
11460	None	5 ksi H2	3	60RC8	60RD1	60RA6
11460	None	10 ksi H2	3	60RA4	60RB9	60RC2
11460	Hydrogen	5 ksi H2	3	60RB11	60RC4	60RD9
11460	Tritium Age 1	5 ksi H2	3	60RA3	60RB8	60RC1
11460	Tritium Age 2	5 ksi H2	3	60RD6	60RA11	60BB4
11460	Tritium Age 3	5 ksi H2	3	60RC9	60RD2	60RA7
11460	Tritium Age 4	5 ksi H2	3	60RB12	60RC5	60RD10

IV. EXPERIMENTAL RESULTS

Type 21-6-9 Brick Forging

Typical Load-Displacement diagrams for arc-shaped specimens in the LT and TL orientations cut from Type 21-6-9 stainless steel and MCN 200787 for the brick forging are shown in Figures 9(a) and 9(b). The load goes through a broad maximum after yielding with a gradual falloff as the crack growth begins and continues to propagate. Similar behavior was observed for arc-specimens taken from the other heat of Type 21-6-9 stainless steel, MCN 200681 as show in Figures 10(a) and 10(b).

The Load-Displacement diagrams for disk-shaped specimens in the LT and TL orientations cut from Type 21-6-9 stainless steel and MCN 200787 for the brick forging are shown in Figures 11(a) and 11(b). These larger specimens failed at higher loads and displacements of the arc-specimens (Figs. 9-10) because the disk-shaped samples are, of course, a different shape and larger in cross-sectional area.

For many of the specimens, crack growth was signaled by a sharp change in the raw data from the potential drop measurements as the specimen resistance changed during loading. Figure 12 shows this for the disk-shaped specimen DTL1-6. Note the step change in resistance, indicated by the left most arrow in Figure 12 at the 18 minute mark. This sudden change in crack length can also be seen in the Change in Crack Length data of Figs 10-11.

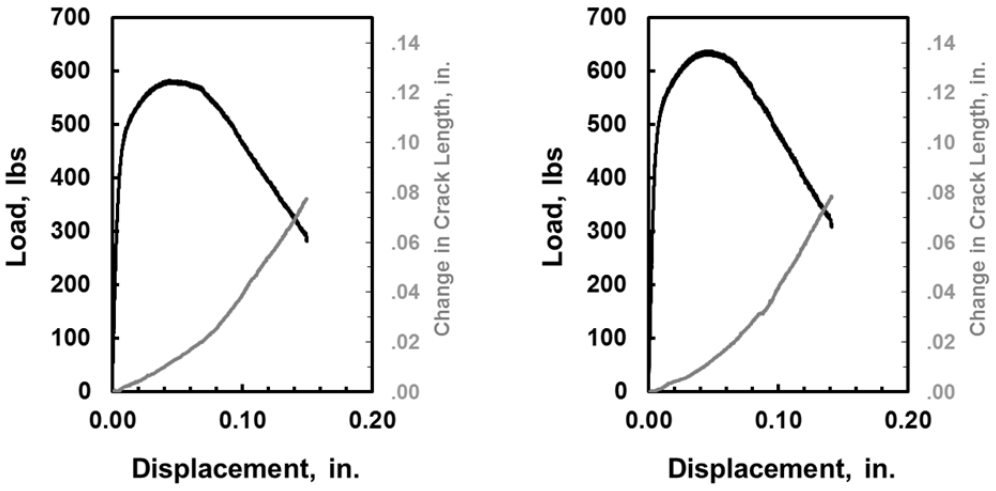

(a) (b)

Figure 9. Typical Load-Displacement and Change in Crack Length Diagrams for Arc-Shaped Specimens Taken from Type 21-6-9 Brick Forging, MCN 200787: (a) LT Orientation (LT122) and (b) TL Orientation (TL132).

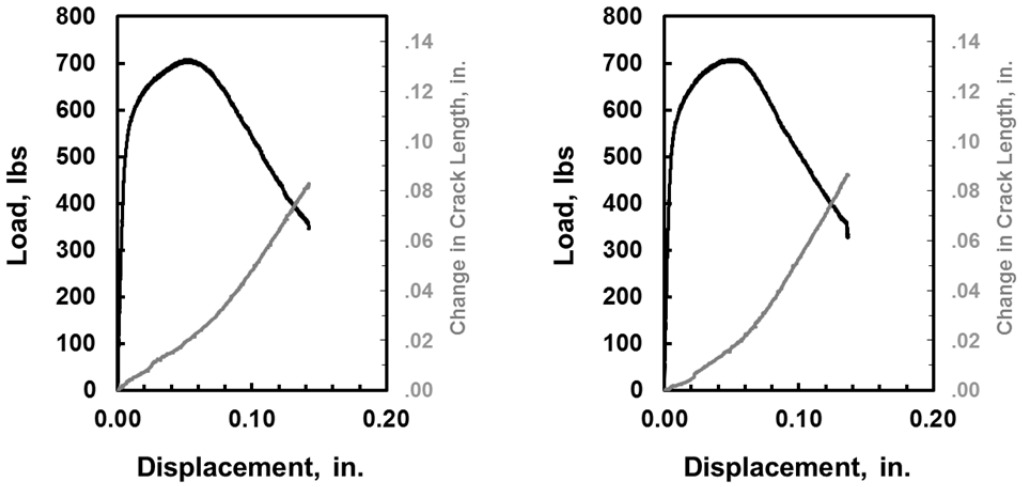

(a) (b)

Figure 10. Typical Load-Displacement and Change in Crack Length Diagrams for Arc-Shaped Specimens Taken from Type 21-6-9 Brick Forging, MCN 200681: (a) LT Orientation (LT251) and (b) TL Orientation (TL251).

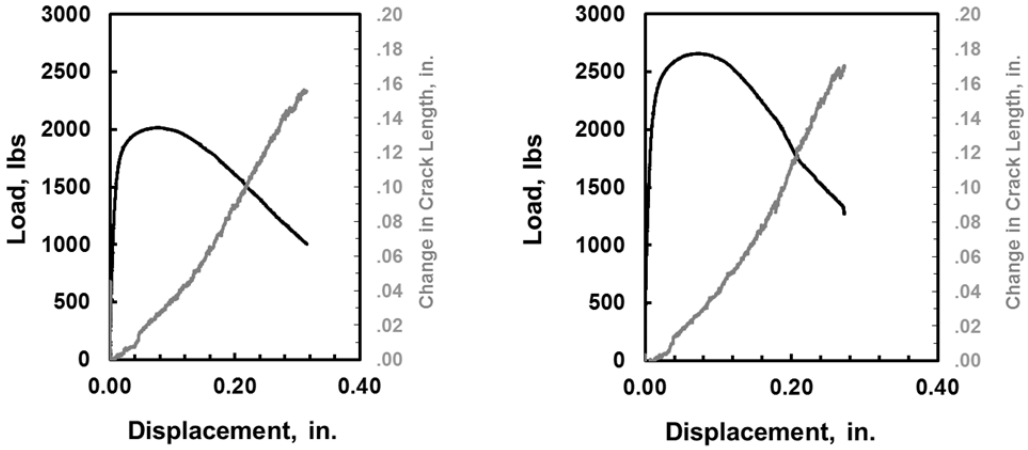

(a) (b)

Figure 11. Typical Load-Displacement and Change in Crack Length Diagrams for Disk-Shaped Specimens Taken from Type 21-6-9 Brick Forging, MCN 200787: (a) LT Orientation (DLT1-6) and (b) TL Orientation (DTL1-6).

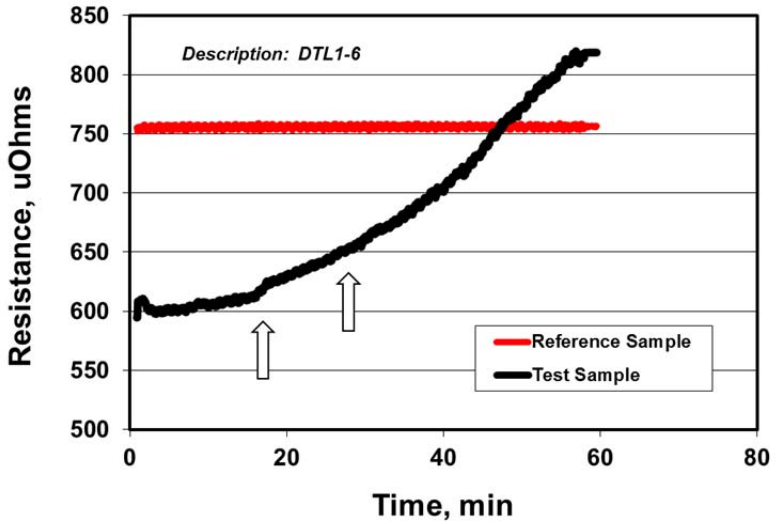

Figure 12. Step Change In Specimen Resistance Raw Data Indicated at Left Arrow at the 18 Minute Mark. The Right Arrow Represents the Point at which the JQ Value was Determined.

As described in the procedure section, the load, displacement, and crack-length data were analyzed per ASTM E1820. Fracture toughness properties are derived from calculating the J-integral, which is calculated from the work of fracture, i.e., the area under the load-displacement diagram and geometric factors that are based on the specimen dimensions and initial crack length. The J-Integral is plotted against the change in crack length and is referred to as the J-R curve. The fracture toughness is that value of the J-integral that is associated with a "significant" amount of crack growth, which is usually taken by an intersection of the J-R curve with an offset line. The slope of the offset line is derived by the material's flow properties and accounts for the change in shape of the crack tip from plastic deformation which occurs before crack extension.

Figures 13-14 show typical J-R curves that were generated for the arc-shaped specimens cut from the two orientations from the Type 21-6-9 brick forging (MCN 200787 and 200683). The results for all of the arc-shaped specimens are listed in Tables VIII-IX. For MCN 200787, the specimens had an average fracture toughness value of 5151± 451 lbs / in the LT orientation and 4948±295 lbs / in in the TL orientation. The fracture toughness values were within one standard deviation and, on average, only different by a few percent. The small effect is most likely due to the relatively small amount of upset that occurs in this rectangular forging.

For MCN 200681, the specimens had an average fracture toughness value of 4748± 432 in the LT orientation and 4472±890 lbs / in in the TL orientation. Again, the values are within one standard deviation of those measured for MCN200787. What is more significant about these fracture toughness values is the fact that they are much higher than the values measured in earlier studies (7, 15) from heats produced in the 1980s and 1990s and taken from forward extruded forgings. In those studies, the fracture toughness values were ~1800-2000 lbs / in for Type 21-6-9 stainless steel.

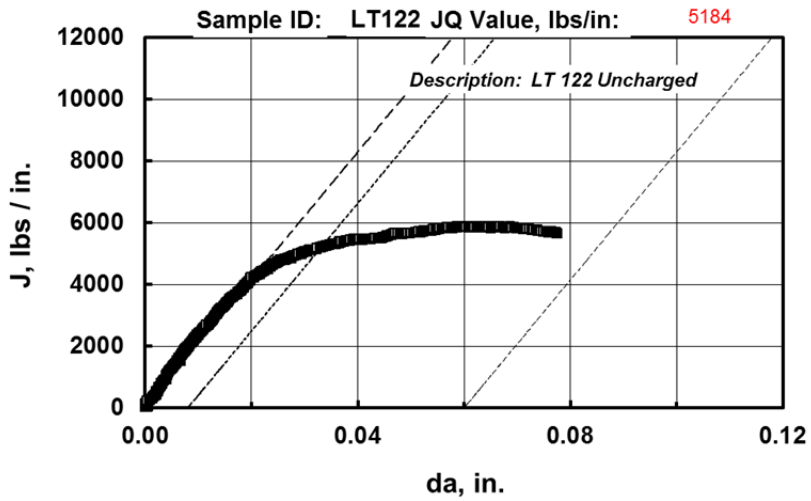

(a)

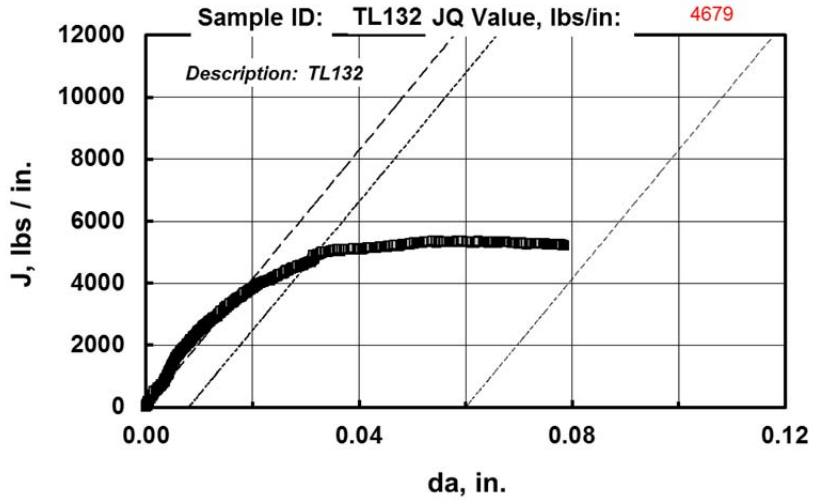

(b)

Figure 13. Typical Fracture Toughness Result for Arc-Shaped Specimens Taken from Type 21-6-9 Brick Forging, MCN 200787: (a) LT Orientation (LT122) and (b) TL Orientation (TL132).

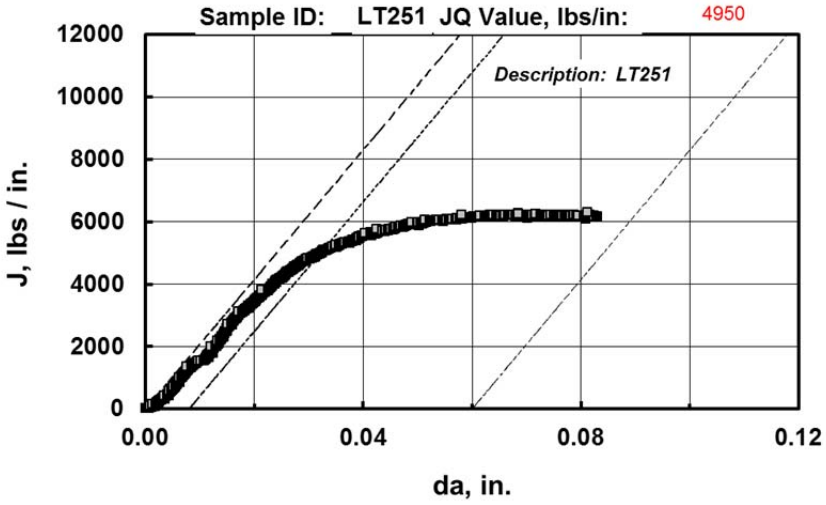

(a)

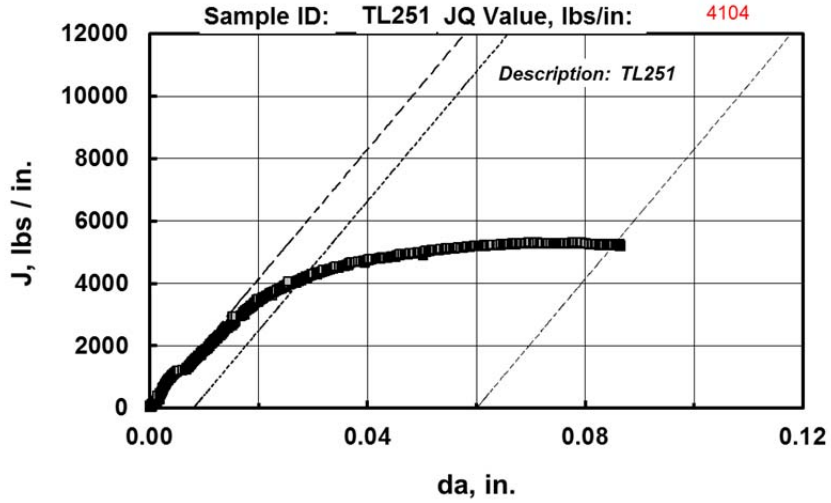

.

(b)

Figure 14. Typical Fracture Toughness Result for Arc-Shaped Specimens Taken from Type 21-6-9 Brick Forging, MCN 200681: (a) LT Orientation (LT122) and (b) TL Orientation (TL132).

Table VIII - Fracture Toughness Properties of Type 21-6-9 Brick Forging Heat 200787 & Arc-Specimen Geometry

Specimen	Condition	JQ, lbs/in		Avg		StDev
LT 122	not charged	5184	LT	5151	±	446
LT 138	not charged	5689				
LT 139	not charged	5133				
LT 1310	not charged	4599				
TL 132	not charged	4679	TL	4948	±	295
TL 134	not charged	5367				
TL 172	not charged	5144				
TL 133	not charged	4810				
TL 173	not charged	4740				
LT 1311	H2-charged	2872	LT	3150	±	264
LT 177	H2-charged	3004				
LT 178	H2-charged	3466				
LT 179	H2-charged	3256				
TL 135	H2-charged	3029	TL	3147	±	220
TL 136	H2-charged	3258				
TL 171	H2-charged	3393				
LT 137	H2-charged	2906				

Figure 15 shows the J-R curves derived for the disk-shaped specimens for MCN 200787 of the Type 21-6-9 forging. The results for the disk-shaped specimens are listed in Table X. The fracture toughness values for the disk-shaped specimens averaged 6994±424 lbs / in in the LT orientation and 7330±1390 lbs / in for specimens cut from the TL orientation. Again, the values are not significantly different from each other. However, two things stand out from the J-R. The fracture toughness values for the disk-shaped specimens are significantly higher and the shape of the J-R curve is steeper. The higher fracture toughness values indicate a significant geometric effect on toughness. These and other forgings may be more resistant to the onset of crack extension and continued crack propagation than is indicated by the J-R data of the sub-size arc specimens.

Table IX - Fracture Toughness Properties of Type 21-6-9 Brick Forging Heat 200681 & Arc-Specimen Geometry

Specimen	Condition	JQ, lbs/in		Avg		StDev
LT 231	not charged	5041	LT	4748	±	432
LT 251	not charged	4950				
LT 271	not charged	4252				
TL 211	not charged	3404	TL	4472	±	890
TL 231	not charged	5000				
TL 251	not charged	4104				
TL 271	not charged	5379				
LT 221	H2-charged	3263	LT	2722	±	454
LT 241	H2-charged	2926				
LT 261	H2-charged	2294				
LT 281	H2-charged	2403				
TL 221	H2-charged	2623	TL	2465	±	531
TL 241	H2-charged	3101				
TL 261	H2-charged	2292				
TL 281	H2-charged	1844				

Table X - Fracture Toughness Properties of Type 21-6-9 Brick Forging Heat 200787 & Disc-Specimen Geometry

Specimen	Condition	JQ, lbs/in		Avg		StDev
DLT 1-3	not charged	7549	LT	6994	±	424
DLT 1-5	not charged	6585				
DLT 1-6	not charged	7083				
DLT 1-8	not charged	6757				
DTL 1-5*	not charged	8598	TL	7330	±	1390
DTL 1-6	not charged	5677				
DTL 1-7	not charged	8355				
DTL 1-8	not charged	6690				
*apparent high yield strength						

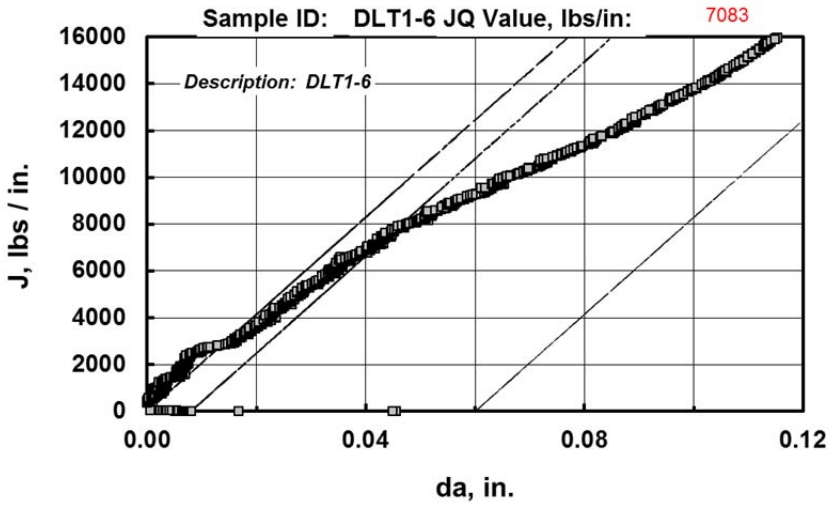

(a)

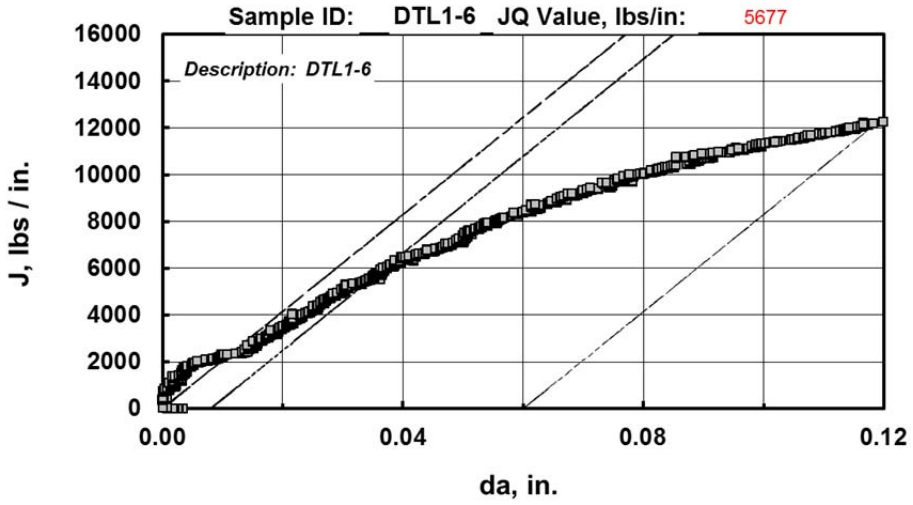

(b)

Figure 15. Typical Fracture Toughness Result for Disk-Shaped Specimens Taken from Type 21-6-9 Brick Forging, MCN 200787: (a) LT Orientation (DLT1-6) and (b) TL Orientation (DTL1-6).

Figure 16 and 17 show typical J-R curves that were generated for the hydrogen-charged arc-shaped specimens cut from the two orientations from the Type 21-6-9 brick forging (MCN 200787). The results are summarized in Tables IX-X. The hydrogen-charged specimens had fracture toughness values that were about 56-62% of the uncharged specimens from the same heat and did not show a strong dependence on crack orientation.

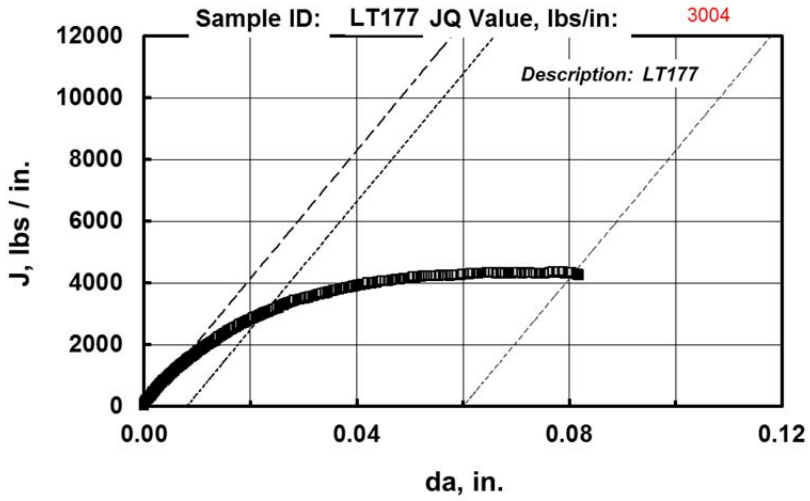

(a)

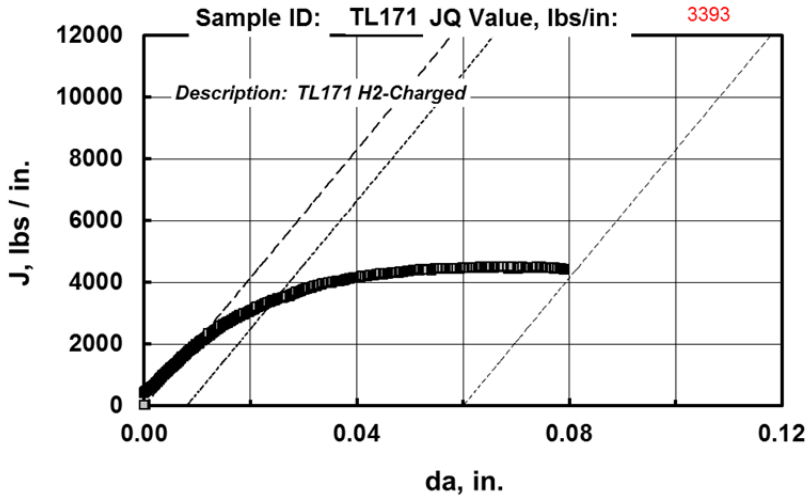

(b)

Figure 16. Typical Fracture Toughness Result for Hydrogen-Charged-Arc-Shaped Specimens Taken from Type 21-6-9 Brick Forging, MCN 200787: (a) LT Orientation (LT177) and (b) TL Orientation (TL171).

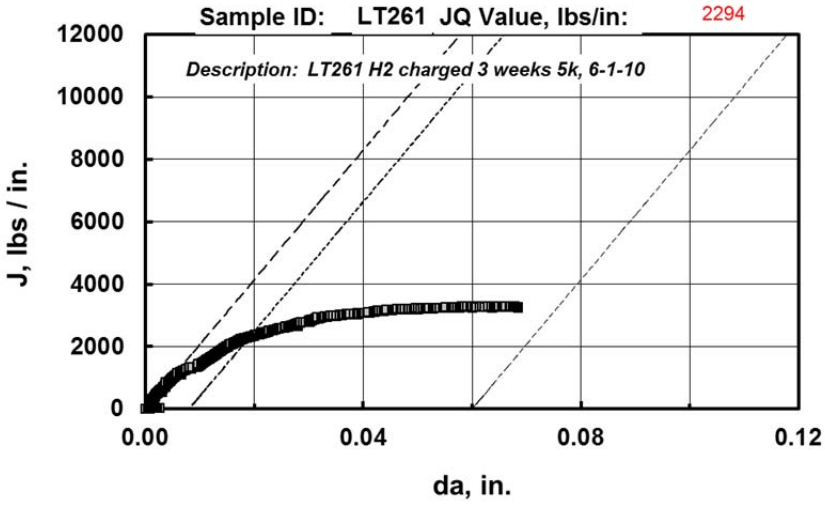

(a)

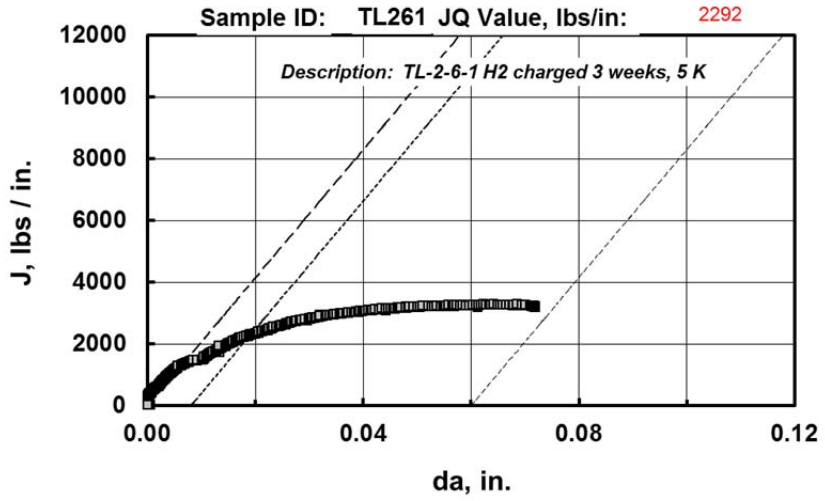

(b)

Figure 17. Typical Fracture Toughness Result for Hydrogen-Charged-Arc-Shaped Specimens Taken from Type 21-6-9 Brick Forging, MCN 200681: (a) LT Orientation (LT261) and (b) TL Orientation (TL171).

Type 316L Stem & Cup Forgings

The fracture toughness properties of these forgings were measured and reported in an earlier report (2). Some of the data is reproduced here because the effect of crack orientation on toughness was included in the earlier work for the Type 316L forgings. Table XI summarizes the results from that study (2).

Multiple tests indicate that the stem forging has an average fracture toughness value of 8681 ± 2304 lbs / in. The high standard deviation is in part because the average value includes specimens from two different locations within the forging. Hydrogen pre-charging reduced the fracture toughness values of the stem to an average value of 6380 ± 968 lbs / in. Thus the hydrogen-precharged specimens have fracture toughness values that average about 73% of the value of the as-forged specimens. The large standard deviation on the average toughness values may call into question this conclusion. However, the conclusion is supported by examining the fracture toughness values of specimens from similar locations. In Table XI, hydrogen pre-charging reduced the toughness of “A” specimens from 10310 lbs / in to 7497 lbs / in or 5788 lbs / in and “B” specimens from 7051 lbs / in to 5854 lbs / in. Note fracture toughness values for specimens taken from the stem section are higher than the cup section of the same forging. The most likely reason for the difference is that the stem portion is strained less than the cup during the forging operation. For the hydrogen precharged specimen taken from the cup forging, Figure 18 indicates a fracture toughness value of 4548 lbs / in. which is less than 60% of the non-charged specimen. Table XI shows that the average value of toughness for the cup forging is 6886 ± 939 lbs / in for non-charged specimens and 4690 ± 135 lbs / in for hydrogen precharged specimens. So for the Type 316L cup forging, hydrogen precharging reduces fracture toughness to a value that is just 68% of the non-charged value. These fracture toughness reductions are large, but the material retains high fracture toughness.

Table XI – Fracture Toughness Values of Stem, Cup, and Block Forgings

Specimens Not Charged				
Specimen	**Source**	**J_Q**	**AVG**	**StDev**
		lbs / in	**lbs / in**	**lbs / in**
26AL11	Stem	10310	8681	2304
26BL13	Stem	7051		
26RC6	Cup	7729	6886	939
26RD8	Cup	5573		
26RE10	Cup	7347		
26RF4	Cup	6895		
59RC1	Block LY	12701	12517	623
59RA1	Block LY	11823		
59RB6	Block LY	13028		
60RC11	Block HY	10551	8562	2813
60RB6	Block HY	6573		
Specimens Pre-Charged with Hydrogen Gas				
Specimen	**Source**	**J_Q**	**AVG**	**StDev**
		lbs / in	**lbs / in**	**lbs / in**
26AL2	Stem	5788	6380	968
26AL8	Stem	7497		
26BL4	Stem	5854		
26RC4	Cup	4548	4690	135
26RD1	Cup	4704		
26RF2	Cup	4817		
59RA9	Block LY	4032	4210	241
59RB2	Block LY	4113		
59RD4	Block LY	4484		
60RA9	Block HY	4202	4344	208
60RB2	Block HY	4246		
60RD4	Block HY	4583		

V. DISCUSSION

In 1996, we reported fracture toughness values of ~1830 lbs / in for high-energy-rate forged Type 21-6-9 stainless steel (7). The forgings in the tests had much higher yield and ultimate strengths (113/165 ksi) than the brick forgings of this study (64/108 ksi) and were conducted using steels manufactured in the late 1980s. In 2007, we reported fracture toughness vales for a conventionally forged Type 21-6-9 forging of ~2000 lbs / in (15). The 2007 forging had yield strengths and ultimate strengths (87/131 ksi) closer to those of the brick forging of this study, which is similar to the forging used by Melcher of LANL (25). Melcher's heat had an average fracture toughness value of 6577±1280 lbs / in. Figure shows a comparison of the J-R curves that Melcher compiled using the 2007 SRNL data and his own data. SRNL used sub-size arc-shaped specimens and LANL used 0.4 inch thick compact tension specimens.

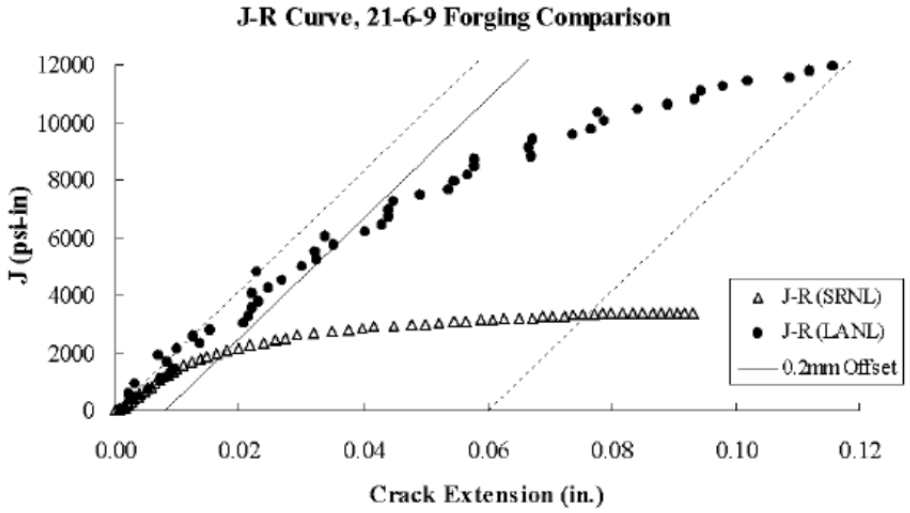

Figure 18. Comparison Between LANL J-R Curve of Brick Forging with SRNL Forward Extruded Cylinder. Large Compact Tension Specimens were used by LANL and Sub-size Arc-Shaped Specimens Used By SRNL (25).

This large difference in fracture toughness values and the comparison shown in Figure 18 suggests that the data from sub-size specimens may be overly conservative. We set out in this study to determine the reasons behind the large fracture toughness differences in the various studies. Three possible factors were of interest: (1) Steel Composition; (2) Forging Type; and (3) Specimen Geometry. Steel composition and forging type were eliminated as a factor by using the same Type 21-6-9 brick forging that LANL used in their study. The brick forging is given a much lower amount of upset than the forward extruded forgings used in the 1996 and 2007 studies (7, 15) and is ideal for this kind of comparison because various sized fracture toughness specimens can be fabricated from it.

The arc-shaped specimen data in this study show that the Type 21-6-9 stainless steel brick forging has much higher fracture toughness than the forward extruded forgings used in the 1996 and 2007 studies (7, 15). The average fracture toughness value for the uncharged steels is ~4829 lbs / in. Thus, a large part of the differences depicted by the J-,R curves of Figure 18 appears to be steel composition and forging type. However, the data of Table X which lists the fracture toughness values from the disk-shaped specimens indicates that there is also an effect of specimen geometry on toughness. The average fracture toughness value of the larger disk-shaped specimens is ~7162 lbs / in, much more in agreement with Melcher's values of ~6577. Figure 19 shows a comparison between one of the larger disk-shaped specimens used in this study with the LANL data of Figure 18. Note that the data indicates that the fracture toughness values from the disk-shaped specimens are in very close agreement with the data from LANL.

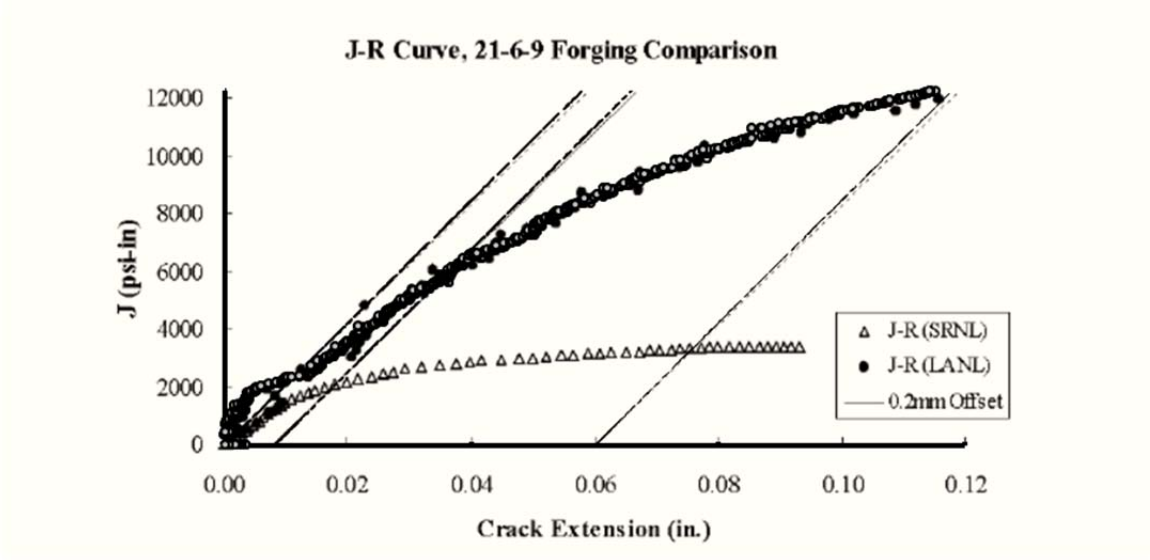

Figure 19. Comparison Between LANL J-R Curve of Brick Forging with SRNL Forward Extruded Cylinder. Specimen DTL1-6 Used for Comparison.

One possible explanation for the higher toughness measured in today's studies is that the Type 21-6-9 stainless steel has a higher nickel content than the steels used in earlier studies. Nickel is well-known toughening agent in steels. The brick forgings used in this study had nickel content greater than 7% by weight (Table I) while the earlier forgings had nickel contents of about 6.2% by weight. Another possible explanation for the high toughness values is the forging process itself. The fact that the cup and brick forgings of this study have high fracture toughness values when compared to the forward extruded cylinders of past studies suggests that forgings with compression type blows result in much better fracture toughness than forgings that are extruded.

Unfortunately, the data from sub-size arc-shaped specimens, which are needed for hydrogen and tritium experiments, still indicate lower fracture toughness values than those measured with larger specimens. The values measured are approximately 67% of those measured with larger specimens, which presumably are more representative of material in a fully constrained reservoir. One possible explanation for the difference is that ductile tearing may be easier when constraint is lost and so cracks begin to grow sooner and propagate easier in sub-size specimens. Three dimensional finite-element modeling may shed light on this question and may help identify how fracture toughness data from sub-size specimens can be adjusted to be more closely aligned with actual material behavior.

There was another interesting observation during the fracture toughness tests conducted in this study that is in agreement with that done at LANL. The J-R curve from LANL shown in Figure 18 shows a deviation at around 2000 lbs / in suggesting that the crack is beginning to grow at that point. LANL did not use potential drop to measure crack extension. Unloading compliance was used instead. The individual data points on their J-R curve represent a compliance measurement and calculated change in crack length based on that compliance change. LANL did in situ microscopy observations of the advancing crack and showed that, indeed, the physical onset of crack extension corresponds to J-Integral values between 2000-2500 lbs / in. This is in agreement with indications shown for much of the J-R data and sample resistance changes. Figures 14, 15 and 17 all suggest that crack actually begins to grow at lower values of the J-Integral than the J_Q value. This has also been observed in prior SRNL tests on tritium exposed samples that show a burst of tritium released at the point apparent crack extension (18).

VI. CONCLUSIONS

The effects of hydrogen, crack orientation, and specimen geometry on the fracture toughness properties of Types 21-6-9 and 316L stainless steels were measured. Brick forgings were used for Type 21-6-9 and Cup forgings for Type 316L. The steels exhibited very high fracture toughness values when compared to the values measure in earlier studies using older heats of steel and forward-extruded forgings. The cracks orientation effect on fracture toughness is largely obscured by the amount of upset that occurred in the forgings. In general, cracks oriented parallel to the forging direction in relatively high upset areas have lower toughness than cracks running perpendicular to the forging direction in areas of low upset. First, fracture toughness properties were measured in Type 316L forgings in the stem and cup sections of the forging.

1. The fracture toughness properties of the Stem, Cup, and Brick forgings are much higher than those measured for forward-extruded experimental forgings and similar steels used in earlier SRNL investigations.

2. Cracks oriented parallel to the forging grain flow propagate easier than those oriented perpendicular to the grain flow. This effect is more pronounced, particularly after hydrogen exposures, when the forging is given a larger upset.

3. Fracture toughness values measured using larger specimens are higher and more representative of the material's actual fracture toughness values. While the toughness properties measured using sub-size specimens are somewhat lower than actual material toughness values, the results are still valuable in that they allow hydrogen and tritium exposures to be conducted at mild temperatures. The sub-size specimen toughness values show the same trends as the larger specimens and are more conservative.

4. Fracture toughness data collected here and at LANL indicate that stable tearing is occurring at J values lower than the ASTM determined JQ values, which are used as a measure of the material fracture toughness value. The significance of this finding is not known and will be explored further in subsequent studies.

VII. FUTURE WORK

Fracture toughness properties for SNL Stem, Cup, and Block forgings will be measured as a function of three different decay helium levels. Fracture tests for two of the decay helium levels are scheduled to begin during FY16. The combined effects on toughness of forging strain rate, forging temperature, tritium, and decay helium will be explored for two different decay helium contents; fracture testing is scheduled to begin in early FY17.

Fracture toughness properties of weld heat-affected zones are being explored with a new study with SNL. Specimens have been prepared by SNL and are being readied for tritium exposures at SRS during FY16. Aluminum Alloys are also being considered for tritium reservoirs and wedge-opening loaded specimens are being prepared for long term in-situ tritium tests.

Finally, Additive Manufacturing is a subject of a Technology Maturation project for evaluating its use for deuterium and/or tritium reservoirs. Fracture toughness values will be measured at SRNL for AM steels before and after exposures to hydrogen isotopes and compared to values measured under the Enhanced Surveillance program. AM plates manufactured using a variety of processes at NSC, LANL, and SNL have been received by SRNL for fracture toughness measurements which will be started in FY16.

VIII. ACKNOWLEDGEMENTS

The author wishes to acknowledge Glenn Chapman and Jim Wilderman for their assistance in preparing specimens and conducting the fracture toughness tests.

IX. REFERENCES

1. Michael J. Morgan and Glenn K. Chapman, “Forging Effects on Fracture Toughness Properties of Tritium-Charged-and-Aged Stainless Steels: Program Plan and Initial Results”, **SRNL-STI-2011-00726,** Savannah River National Laboratory, Aiken, SC, November, 2011.

2. Michael J. Morgan, “Fracture Toughness Properties of Forged Stainless Steels – Effect of Hydrogen, Forging Strain Rate, and Forging Temperature”, **SRNL-STI-2015-00103,** Savannah River National Laboratory, Aiken, SC, February 2015.

3. Michael J. Morgan, “Hydrogen Fracture Toughness Tester Completion”, **SRNL-STI-2015-00518**, Savannah River National Laboratory, Aiken, SC, September 2015.

4. G. R. Caskey, Jr., "Hydrogen Effects in Stainless Steels", *Hydrogen Degradation of Ferrous Alloys*, ed. J. P. Hirth, R. W. Oriani, and M. Smialowski, eds., (Park Ridge, NJ: Noyes Publication, 1985), p. 822.

5. S. L. Robinson, "The Effects of Tritium on The Flow and Fracture of Austenitic Stainless Steels", *Proc. Fourth Int. Conf. on Hydrogen Effects on Material Behavior*, A. W. Thompson and N. R. Moody, eds., The Minerals, Metals & Materials Society, Warrendale, PA, 1989, p. 433.

6. S. L. Robinson and G. J. Thomas, “Accelerated Fracture due to Tritium and Helium in 21-6-9 Stainless Steel”, *Metallurgical Transactions A*, 22A (1991), 879-885.

7. M. J. Morgan and M. H. Tosten, “Tritium and Decay Helium Effects on the Fracture Toughness Properties of Types 316L, 304L, and 21Cr-6Ni-9Mn Stainless Steels”, *Hydrogen Effects in Materials*, ed. A. W. Thompson and N. R. Moody, (Warrendale, PA: TMS, 1996), p. 873.

8. M. Tosten and M. Morgan, “Transmission Electron Microscopy Study of Helium-Bearing Fusion Welds”, *2008 International Hydrogen Conference – Effect of Hydrogen on Materials*, Brian Somerday, Petros Sofronis, and Russel Jones, eds., (ASM International, Materials Park, OH, 2009), pp 694-701.

9. Michael J. Morgan, “Hydrogen Effects on the Fracture Toughness Properties of Forged Stainless Steels”, *Proceedings of PVP2008 2008 ASME Pressure Vessels and Piping Division Conference*, July 27-31, 2008, Chicago, Illinois USA

10. Michael J. Morgan, “Tritium Aging Effects on the Fracture Toughness Properties of Forged Stainless Steels”, *Proceedings of the Conference on Materials Innovations in an Emerging Hydrogen Economy*, February 24-27, 2008, Cocoa Beach, Florida.

11. Michael J. Morgan, Scott L. West, and Michael H. Tosten, "Effect of Tritium and Decay Helium on the Fracture Toughness Properties of Stainless Steel Weldments", *Proceedings of the 8th International Conference on Tritium Science and Technology*, September 16-21, 2007, Rochester, New York, Walter T. Shmayda, ed., *Fusion Science and Technology*, Vol. 54, No. 2, August 2008, pp 501-505.

12. M. H. Tosten and M. J. Morgan, "Microstructural Study of Fusion Welds in 304L and 21Cr-6Ni-9Mn Stainless Steels", **WSRC-TR-2004-00456**, Savannah River National Laboratory, Washington Savannah River Company, Savannah River Site, Aiken, SC, March, 2005.

13. M. H. Tosten and M. J. Morgan, "Transmission Electron Microscopy Study of Helium-Bearing Fusion Welds", **WSRC-TR-2005-00477**, Savannah River National Laboratory, Washington Savannah River Company, Savannah River Site, Aiken, SC, November, 2005.

14. M. J. Morgan, M. H. Tosten, and S. L. West, "Tritium Effects on Weldment Fracture Toughness", **WSRC-TR-2006-00257**, Savannah River National Laboratory, Washington Savannah River Company, Savannah River Site, Aiken, SC, August 10, 2006.

15. M. J. Morgan, S. L. West, and G. K. Chapman, "Tritium Aging Effects on Fracture Toughness of Type 21-6-9 Stainless Steel", **WSRC-TR-2007-00244**, Savannah River National Laboratory, Washington Savannah River Company, Savannah River Site, Aiken, SC, June 14, 2007.

16. M. J. Morgan and G. K. Chapman, "Hydrogen Effects on the Fracture-Toughness Properties of Type 316L Stainless Steel", **WSRC-TR-2007-00479,** Savannah River National Laboratory, Washington Savannah River Company, Savannah River Site, Aiken, SC, December 17, 2007.

17. Michael J. Morgan and Glenn K. Chapman, "Hydrogen Effects on the Fracture Toughness Properties of Type 316L Stainless Steel From -100º C to +150º C", **SRNL-TR-2008-00317**, Savannah River National Laboratory, Aiken, SC, December 2008.

18. M. J. Morgan and G. K. Chapman, "Cracking Thresholds and Fracture Toughness Properties of Tritium-Charged-and-Aged Stainless Steels", **WSRC-TR-2010-00393**, Savannah River National Laboratory, Washington Savannah River Company, Savannah River Site, Aiken, SC, December, 2010.

19. Michael J. Morgan and Glenn K. Chapman, "Hydrogen Effects on the Fracture-Toughness Properties of Types 304L AND 21-6-9 Stainless Steels From 173 K to 423 K", **SRNL-TR-2009-00468,** Savannah River National Laboratory, Aiken, SC, December 2009.

20. M. J. Morgan and D. Lohmeier, "Threshold Stress Intensities and Crack Growth Rates In Tritium-Exposed HERF Stainless Steels", *Hydrogen Effects on Material Behavior*, N. R. Moody and A. W. Thompson, eds., pp. 459-468, TMS, Warrendale, PA (1990).

21. M. J. Morgan "The Effects of Hydrogen Isotopes and Helium on the Flow and Fracture Properties of 21-6-9 Stainless Steel", *Proc. Fine Symposium*, ed. P. K. Liaw, J.R. Weertman, H. L. Marcus, and J. S. Santner, (Warrendale, PA: TMS, 1990), 105-111.

22. M. J. Morgan and M. H. Tosten, "Microstructure and Yield Strength Effects on Hydrogen and Tritium Induced Cracking in HERF Stainless Steel", *Hydrogen Effects on Material Behavior*, ed. N. R. Moody and A. W. Thompson, (Warrendale, PA: TMS, 1990), 447-457.

23. M. J. Morgan and M. H. Tosten, "Tritium and Decay Helium Effects on Cracking Thresholds and Velocities in Stainless Steels", Fusion Technology, Vol. 39, pages 590-595, 2001.

24. Y. Kim, Y. J. Chao, M. J. Pechersky, M. J. Morgan, "C-Specimen Fracture Toughness Testing: Effect of Side Grooves and η Factor", *Journal of Pressure Vessel Technology*, August 2004, Vol. 160 page 293.

25. Ryan Melcher, "7K0004 Forging Fracture Toughness Test Report", WT-1-2007-008 (U), Rev. A, March 20, 2008, LANL, New Mexico.

26. C. San Marchi, B.P. Somerday and S.L. Robinson, "Permeability, Solubility and Diffusivity of Hydrogen Isotopes in Stainless Steels at High Gas Pressures", *International Journal of Hydrogen Energy*, Volume 32, Issue 1, January 2007, 100-116.

27. ASTM E647-95a "Standard Test Method for Measurement of Fatigue Crack Growth Rates", *1999 Annual Book of ASTM Standard Volume 3.01 Metals-Mechanical Testing; Elevated and Low-Temperature Tests; Metallography*, American Society for Testing and Materials, 1999.

28. ASTM E1820-99 "Standard Test Method for Measurement of Fracture Toughness", *1999 Annual Book of ASTM Standard Volume 3.01 Metals-Mechanical Testing; Elevated and Low-Temperature Tests; Metallography*, American Society for Testing and Materials, 1999.